Front. Optoelectron. 2013, 6(4): 359–372
DOI 10.1007/s12200-013-0346-6

REVIEW ARTICLE

Monolithic all-solid-state dye-sensitized solar cells

Yaoguang RONG[1], Guanghui LIU[1], Heng WANG[1], Xiong LI[1,2], Hongwei HAN (✉)[1]

1 Michael Grätzel Center for Mesoscopic Solar Cells, Wuhan National Laboratory for Optoelectronics, School of Optical and Electronic Information, Huazhong University of Science and Technology, Wuhan 430074, China
2 College of Materials Science and Engineering, Huazhong University of Science and Technology, Wuhan 430074, China

Abstract As a low-cost photovoltaic technology, dye-sensitized solar cell (DSSC) has attracted widespread attention in the past decade. During its development to commercial application, decreasing the production cost and increasing the device stability take the most importance. Compared with conventional sandwich structure liquid-state DSSCs, monolithic all-solid-state mesoscopic solar cells based on mesoscopic carbon counter electrodes and solid-state electrolytes present much lower production cost and provide a prospect of long-term stability. This review presents the recent progress of materials and achievement for all-solid-state DSSCs. In particular, representative examples are highlighted with the results of our monolithic all-solid-state mesoscopic solar cell devices and modules.

Keywords photovoltaic (PV) technology, monolithic, dye-sensitized solar cells (DSSCs), all-solid-state, mesoscopic, carbon counter electrode

1 Introduction

Photovoltaic (PV) technology has been realized as a suitable renewable power source for the fulfillment of increasing world energy consumption with the least impact on the environment. In the history of this technology, solid-state junction devices, usually made of silicon, dominate the commercial market. However, the dominance of the PV field by inorganic solid-state junction devices is now being challenged by the emergence of a third generation of cells such as dye-sensitized solar cells (DSSCs). DSSCs are very attractive because they could be fabricated from materials that do not need to be highly purified and by low-cost printing procedures. Besides, DSSCs are unique compared with almost all other kinds of solar cells, which realize that the electron transport, light absorption and charge separation processes are each handled by different materials in the device [1–3]. Conventional DSSCs are based on a sandwich structure comprising of two conducting glass substrates, between which contains a liquid-state electrolyte. The highest power conversion efficiency (PCE) for DSSCs based on this structure has reached to over 12% [4–6]. However, to realize the commercialization of DSSCs, it depends not only on the ability to increase the PCE, but also on the development of ultralow-cost architectures that are stable over 20 years. To compete with other PV technology, commercializing 10%-efficient modules may require ultralow-cost architectures that reduce inherent costs by removing at least one glass substrate which accounts for most of materials cost [7,8]. Besides, the liquid-state electrolyte containing volatile solvent is also an issue for the commercial applications of DSSCs.

In this review, we mainly focus on monolithic all-solid-state DSSCs, which offer a prospect of being lower cost and require simpler manufacturing process. Eliminating the second conducting glass substrate and using carbon counter electrode (CE) instead of noble metal CE, the material cost of this design decreased largely compared with conventional sandwich structure liquid-state DSSCs. Due to the solid-state electrolyte, the devices and modules present excellent stability and durability. All these values make the design a promising path for the commercialization of DSSCs.

Received May 23, 2013; accepted June 8, 2013

E-mail: hongwei.han@mail.hust.edu.cn

2 Structure and working principle of DSSCs

DSSCs mainly consist of three major components: the working electrode which is usually a dye molecule attached nanocrystalline porous film deposited on conducting glass substrate, the CE which is often a platinized conducting glass substrate and the electrolyte containing a redox couple. Figure 1 shows the structure and working principle of DSSC. The sensitizer of dye in a DSSC is anchored to a wide-bandgap semiconductor such as TiO_2

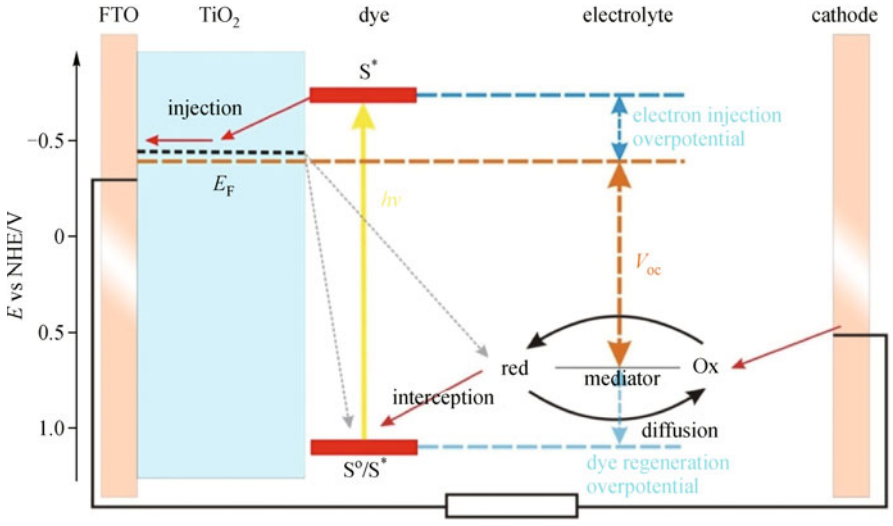

Fig. 1 DSSC schematic and operation

[1], SnO_2 or ZnO [9] on FTO (fluorine-doped tin oxide) glass. When the dye absorbs light, the photoexcited electron rapidly transfers to the conduction band of the semiconductor, which carries the electron to one of the electrodes. A redox couple, usually comprised of iodide/triiodide (I^-/I_3^-), then reduces the oxidized dye back to its neutral state and transports the positive charge to the platinized counter-electrode. The iodide is regenerated in turn by the reduction of triiodide at the CE. The voltage generated under illumination corresponds to the difference between the Fermi level of the electron in the semiconductor and the redox potential of the electrolyte. Overall, the device generates electric power from light without suffering any permanent chemical transformation.

3 Monolithic all-solid-state DSSCs

3.1 Monolithic structure for DSSCs

In 1996, Kay and Grätzel showed that porous carbon electrodes function well as CEs in DSSCs [10]. The catalytic and conducting properties were obtained through the combination of conducting graphite and catalyzing carbon black powders. This opened for a single-substrate monolithic triple-layer structure for DSSCs, consisting of a nanocrystalline/nanoporous TiO_2 film, an insulating/spacer ZrO_2 layer, and the above-mentioned carbon layer. Figure 2 shows the structure of a typical monolithic liquid-state DSSC. Though the efficiency obtained with the monolithic concept device was somewhat lower than that with a double-substrate sandwich structure devices, a promising efficiency of 6.7% at full sun irradiation ($1000\ W \cdot m^{-2}$) with respect to the active TiO_2 surface, was obtained with test cells ($0.4\ cm^2$) using an acetonitrile-based electrolyte in combination with basic laboratory manufacturing techniques, such as manual patterning of the transparent conducting layer and manual application of the electrode layers.

In 1998, Bach and coworkers first used gold CE and a solid-state medium Spiro-OMeTAD to assemble mono-

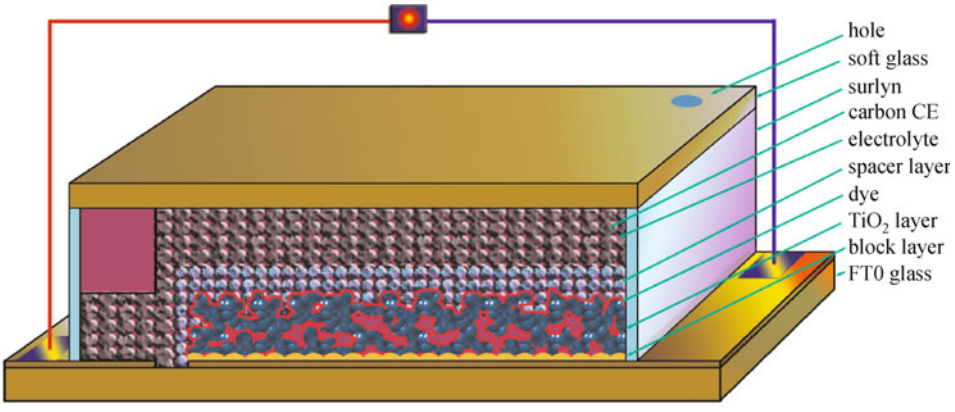

Fig. 2 Structure of typical monolithic liquid-state DSSC

lithic all-solid-state DSSC device [11]. The structure of monolithic all-solid-state DSSC is shown in Fig. 3. Being different from monolithic DSSCs based on carbon CE, this design employed gold CE instead of carbon CE, which is deposited on the solid-state electrolyte. After that, monolithic all-solid-state DSSCs attracted much more attention [12–15] and the efficiency has reached over 10% [16–18], which is comparable with that achieved by traditional sandwich structure liquid-state DSSCs.

In 2009, Han and coworkers developed a monolithic all-solid-state DSSC based on mesoscopic carbon CE [19]. The structure of the device is shown in Fig. 4. This design integrates the advantages of monolithic concept and solid-state electrolyte for DSSCs. All the layers are screen printed on a single substrate. The porous structure of the layers favors the infiltration of solid-state electrolyte and benefits the contact between the electrolyte and working electrode interfaces. For the all-solid-state devices, the sealing process would be also much simpler. Since there is no risk of leakage of the electrolyte, the device or module becomes suitable for indoor applications, and is even portable.

3.1.1 CEs

For DSSCs, CEs are employed for collecting electrons and transferring electrons to electrolyte. When the device works with a high current density ($>20\ \mathrm{mA\cdot cm^{-2}}$), the conductivity and electrochemical catalytic activity of CEs would affect the performance of the device importantly. Up to now, in traditional sandwich-structure DSSCs, platinum CEs present excellent catalytic activity toward I^-/I_3^- electrolyte and high conductivity, this makes it the most promising CE material [5]. However, for monolithic DSSCs, platinum CEs could not be used as for conventional sandwich structure DSSCs. Since the working electrodes (WEs) and CEs are constructed on a single conducting glass substrate, the CEs should be porous for the infiltration of dye solution and electrolyte. In theory, we could use platinum particles to obtain a porous film, but the amount of the platinum used for porous film is too large. For a porous platinum film with thickness of about 50 nm would need $1\ \mathrm{g\cdot m^{-2}}$ platinum, which is nearly 100 times as much as platinum CEs used in sandwich structure DSSCs. Thus, abundant available low-cost materials should be developed for CEs of monolithic DSSCs.

It is well known that carbon materials are widely used in the field of printing, electronics, energy, and so on. Carbon materials own the properties of good conductivity, high electrochemical catalytic activity, simple fabricating procedures and low price, which make it the best choice for CEs in all kinds of commercial applications. In 1996, Kay and Grätzel first reported a novel low-cost type of monolithic DSSC based on cheap graphite/carbon black electrode [10]. The carbon CEs are fabricated by screen printing on the insulating/spacer layer, and then, sintered in air condition to eliminate the cellulose. This could increase the porosity of the CEs for the infiltration of dye solution and electrolyte.

The catalytic activity of the CEs for triiodide reduction as well as their conductivity may be considerably enhanced by adding about 20% of carbon black to the dispersion of graphite powder. The enhanced catalytic activity is due to the very high surface area of carbon black, while the improved conductivity results from the partial filling of large pores between the graphite flakes with smaller carbon black aggregates.

For good cohesion between the graphite particles and carbon black, a binder is required, which also enhances the adhesion of the CE to the underlying layer. This binder should withstand firing at 450°C in air, which is the usual heat treatment of the photo-electrode to create a virgin, dehydroxylated TiO_2 surface for dye adsorption. Organic polymers, even heat resistant ones like polyimide,

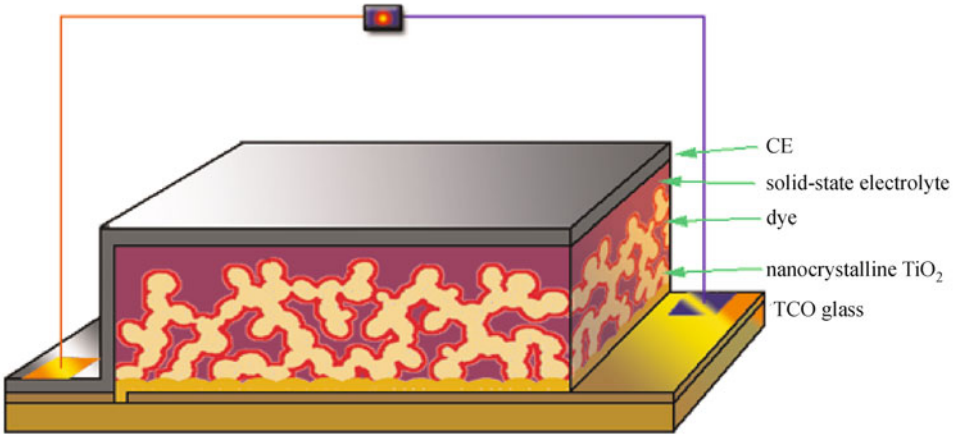

Fig. 3 Structure of typical monolithic all-solid-state DSSC

polyethyleneimine or poly-acrylonitrile are not suited, since they liberate volatiles that poison the nearby TiO_2 photoelectrode. A binder that is well compatible with the other components of the DSSC and adheres well to carbon is in fact TiO_2 itself.

CEs prepared by doctor blading of an aqueous dispersion of graphite powder, 20% by weight of high surface area carbon black and 15% nanocrystalline TiO_2 with a particle size below 20 nm are well adherent and scratch resistant after firing in air at 450°C for 10 min. To obtain a sheet resistance of 5 Ω, a thickness of 50 μm is required. The resistance increases to about twice this value after soaking with electrolyte due to swelling of the carbon layer. Thanks to their open porous structure and a surface roughness factor in excess of 1000 such carbon CEs are as active for triiodide reduction as the conventional platinum electrodes.

In 2009, Skupien and coworkers developed a polyol process as a low cost method to fabricate thermally stable SnO_2: Sb/Pt and carbon black/Pt nanocomposites [20]. The catalytic and electric properties of these materials were compared with a new platinum-free type of carbon CE. The layers containing low platinum amounts (less than 5 $\mu g \cdot cm^{-2}$) exhibit a very low charge transfer resistance of about $0.4\ \Omega \cdot cm^{-2}$. Also the conductive carbon layer shows an acceptable charge transfer resistance of $1.6\ \Omega \cdot cm^{-2}$. Additionally, the catalytic layer containing porous carbon black reveals excellent sheet resistance below $5\ \Omega \cdot square^{-1}$. This feature has enabled to work out a low cost CE, which combined suitable catalytic and conductive properties.

In 2009, Han group reported a new method to platinized carbon black and developed a mesoscopic platinized carbon electrode [19]. In 2012, the electrochemical characterization and photoelectric behavior of the electrode were investigated particularly [21]. Mesoscopic platinized carbon electrode for monolithic DSSC was developed by thermal deposition. The results indicated the catalytic activity and the lateral conductivity of the mesoscopic graphite/carbon black CE were improved by introducing trace of platinum. High energy conversion efficiency of up to 7.61% was obtained for monolithic DSSC based on the mesoscopic platinized carbon CE. The surface pattern of the mesoscopic platinized carbon film is presented in Fig. 5 with the scanning electron microscopy (SEM) image, exhibiting mesoscopic film with multi-pores. The Brunauer-Emmett-Teller (BET) test indicated that the surface area of this porous layer is $91.08\ m^2 \cdot g^{-1}$, the Barrett-Joyner-Halenda (BJH) average pore diameter and pore volume are 14.7 nm and $0.33\ cm^3 \cdot g^{-1}$, respectively. This means that a mesoscopic platinized carbon later of $1.2\ cm^2$ geometric area and 50 μm thickness has an active surface area of $3825\ cm^2$ and a porosity of 24%. When the Pt content is low (0.5%), the homogeneously dispersed Pt nanoparticles and porous structure would ensure that this mesoscopic carbon electrode supplied considerable quantities of catalytic active sites to improve the process of electron exchange between electrode and electrolyte. However, with Pt content increasing, it can be found that the small Pt particles moved to the back-fence particles and aggregated together to form a large bulk with the Pt percent increase. At the same times, with the bulk growing up, some of the pores in the mesoscopic carbon substrate were blocked.

To distinguish the differences of catalytic activity before and after depositing different Pt content on the mesoscopic carbon CE, CV curves of the mesoscopic carbon CEs with different Pt percents were characterized at a scan rate of $100\ mV \cdot s^{-1}$ and presented in Fig. 6. It could be found that there were two typical pairs of redox waves. The more negative pair is assigned to redox reaction (1) and the more positive one is appointed to redox reaction (2).

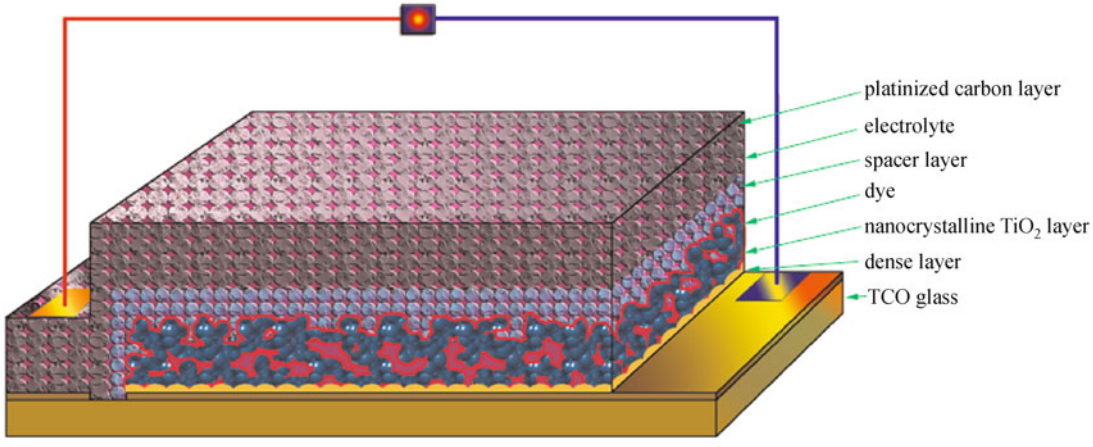

Fig. 4 Structure of typical monolithic all-solid-state DSSC based on mesoscopic carbon CE [19]

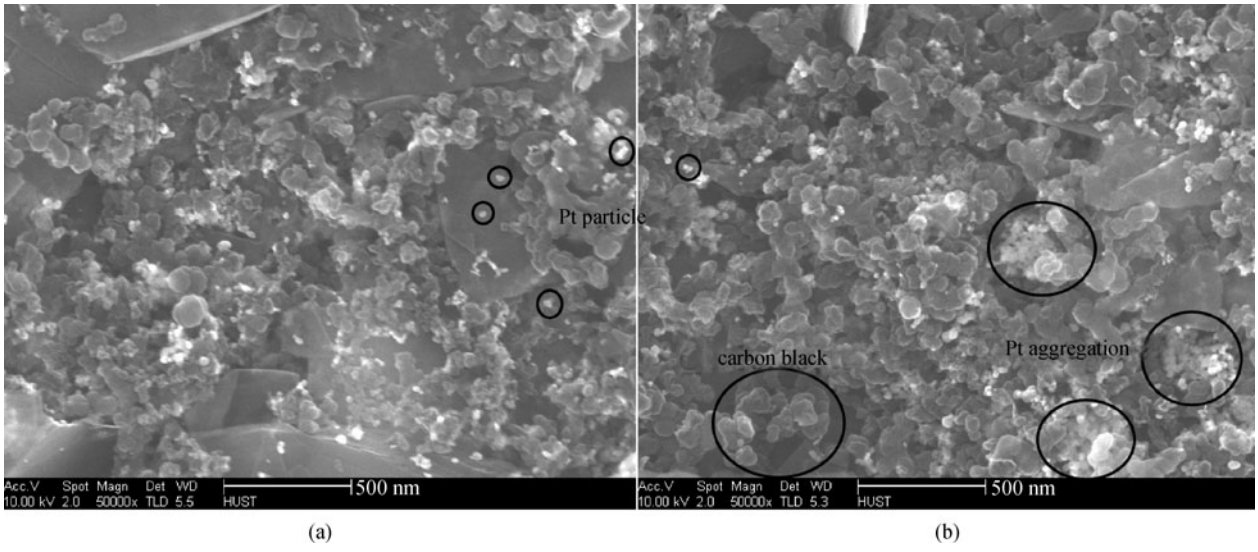

Fig. 5 SEM images of mesoscopic carbon film modified with platinum (a) 0.5 wt. % and (b) 3wt. % [21]

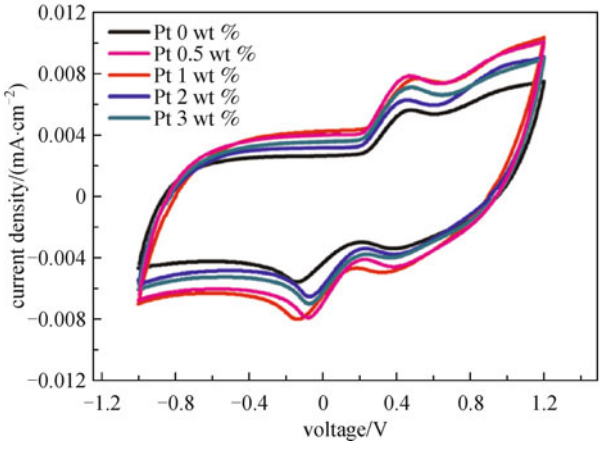

Fig. 6 CV data of carbon electrode containing different amount of platinum particles [21]

$$I_3^- + 2e^- = 3I^-, \quad (1)$$

$$3I_2 + 2e^- = 2I_3^-. \quad (2)$$

Generally, it could be expected that the percent of Pt in carbon film should be as high as possible for higher catalytic activity. However, in the case of the platinized carbon electrodes, the electrode with 0.5% Pt loading shows the highest catalytic activity. When the percent of Pt in mesoscopic carbon film increased from 0.5% to 3%, the catalytic activity decreased slightly owing to the decline of electrochemical active surface area.

3.1.2 Spacer layer

For monolithic DSSCs, the spacer layer influences the photovoltaic performance of the devices significantly. Spacer layer functions to insulate the working electrode and CE and provide space for electrolyte to diffuse. Besides, the existence of spacer layer could reflect some light that has not been utilized by the sensitized working electrode.

To increase the short circuit current density J_{sc} and overall conversion efficiency of the device, the distance between the working electrode and CE should be minimized. Thus, minimizing the thickness of the spacer layer is the most obvious possibility, and is in particular attractive for the monolithic cell concept. Hinsch and coworkers investigated the influence of the spacer layer on the limiting J_{sc} [22]. By assuming a linear correlation between the diffusion-limited current and the concentration of the I_3^- in the redox electrolyte, the effective diffusion coefficient and the corresponding porosity (0.7 and 0.8 for TiO_2 and ZrO_2, respectively) as well as the matrix factors (18 and 50 for TiO_2 and ZrO_2, respectively) have been derived from our measurements. Based on these data, the diffusion limitation of the short circuit current has been calculated as a function of electrode spacing. As could be found from Fig. 7, a pure iodide-based molten salt electrolyte, at room temperature, can provide a reasonable short circuit current of 15 $mA \cdot cm^{-2}$ only for electrode distances smaller than 10 μm.

3.2 Monolithic all-solid-state DSSCs

It is well known that the use of volatile solvent in the liquid-state electrolyte usually results in the problems of leakage, dye desorption, electrode corrosion, and so on. Replacing the liquid electrolyte by a solid-state medium, such as hole conductors and polymer electrolyte, seems to be a solution to these problems. Classified by structure, all-solid-state DSSCs could be divided into monolithic all-

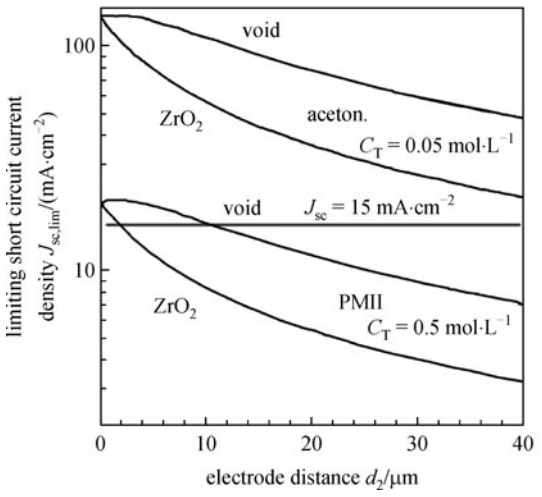

Fig. 7 Calculations of diffusion-limited short circuit current in DSSC in standard cell configuration, which is a photoelectrode consisting of 10 μm TiO_2 active layer and 7 μm ZrO_2 back-scattering layer and a platinized CE, as a function of the electrode distance. Notification: "void" corresponds to the situation without ZrO_2 layer. The circles indicate equal current density. The calculations for a low viscous electrolyte which is diluted with highly volatile acetonitrile are given as a reference. A cell temperature of 25°C is assumed, the concentration C_T of I_3^- is 0.5 mol·L^{-1} in the case of the PMII (propylmethylimidazolium) molten salt electrolyte and 0.05 mol·L^{-1} for the reference electrolyte [22]

solid-state DSSCs and sandwich structure all-solid-state DSSCs. Compared with sandwich structure all-solid-state DSSCs, monolithic all-solid-state DSSCs use only one conducting glass substrate, which owns the advantages of low cost, simple fabrication procedures and easy to large scale manufacturing. Up to now, monolithic all-solid-state DSSCs employs noble metals, carbon materials, and metal composites for CEs.

3.2.1 Monolithic all-solid-state DSSCs based on metal CEs

Monolithic all-solid-state DSSCs based on metal CEs usually employ gold or silver as the electrode material. The fabrication process is presented as follows:

1) Laser scribing of the FTO conducting glass substrate;
2) Deposition of a layer of dense TiO_2;
3) Printing TiO_2 working electrode layer;
4) Dye processing;
5) Pore filing of solid-state organic hole transport materials;
6) Deposition of noble metal based CE on the organic hole transport materials.

Hole transport materials (HTM) can be divided into two classes, organic hole transport materials such as Spiro-OMeTAD, P3HT, PEDOT, and inorganic transport materials such as CuI, CuSCN and $CsSnI_3$. Up to now, most researches focus on monolithic all-solid-state DSSCs based on noble metal CEs using Spiro-OMeTAD and P3HT as the HTMs.

Organic hole conductors Spiro-OMeTAD is the super star material for the HTM in all-solid-state DSSCs. As early as in 1998, Bach and coworkers [11] first used the organic hole conductor Spiro-OMeTAD as the electrolyte to assemble all-solid-state DSSC device and obtained an efficiency of 0.73%. In 2001, Grätzel group used TBP and Li $[CF_3SO_2]_2N$ to decrease the electron recombination between TiO_2 and Spiro-OMeTAD, and enhanced the efficiency to 2.56% [23]. In 2002, Krüger and coworkers used Ag^+ to treat the dye of N719 [24]. This increased the light absorption and decreased the recombination, which leaded to an increase of the overall efficiency to 3.2%. In 2005, Schmidt-Mende and coworkers employed a dye coded Z907 instead of the dye of N719 for the device, and enhanced the efficiency to 4% [25]. At the same time, Schmidt-Mende and coworkers first used organic dye coded D102 to achieve an efficiency of 4.1% [26]. Compared with traditional Ru based dyes such as N719 and Z907, organic dyes own the advantages of much simpler synthesizing procedures, more choices for the raw materials and higher molar extinction coefficiency. In 2007, Snaith and coworkers used the dye of K68 and silver CE to assemble all-solid-state DSSCs [13]. The efficiency was enhanced to 5.1%. The groups in the dye of K68 had the ability to optimize the ions and decrease the recombination. Thus, the V_{oc} and J_{sc} were enhanced. Compared with gold CE, silver CE could reflect the incident light, thus increases the light collecting ability and the J_{sc}. During the later years, the efficiency of all-solid-state DSSCs based on Spiro-OMeTAD stays around 5%. Until 2011 Cai and coworkers employed a new sensitizer coded C220 for the device and enhanced the efficiency to 6.08% [27]. C220 is a kind of organic dye. Compared with Z907, this dye presented higher molar extinction coefficiency. Based on this dye, the device showed much high electron collection efficiency. In the same year, Burschka and coworkers employed the dye coded Y123 and additive coded FK102 into the device [28]. The efficiency was enhanced to 7.2%. This is the highest efficiency for all-solid-state DSSCs based on organic HTMs.

The absorption capacity of Y123 is a little weaker than that of C220, while these two sensitizers have no significant difference in UV-vis absorption spectrum. However, the donor unit in Y123 molecule is bigger than C220, which contributes to the action range between dye molecule and Spiro-OMeTAD and hinders recombination of electron and hole, thus leading to enhanced electron collection efficiency.

A p-type dopant FK102 can improve the conductivity of Spiro-OMeTAD and accordingly increase the fill factor of all-solid-state DSSCs. Compared with traditional photo-doping, chemical doping is easier to control with better repeatability. The efficiency of all-solid-state DSSCs based on Spiro-OMeTAD is still far from that of conventional

liquid DSSCs. The main reason is that, the light absorption layer of the former cells is only around 2 μm, which renders low incident light utilization efficiency. However, if the thickness of the nanocrystalline layer increased, the filling degree of solid-state electrolyte will decrease, resulting in low electron collection efficiency. Therefore, further work for improvement will focus on developing new dyes with more broad absorption spectrum and higher molar absorption coefficient, and searching for more efficient filling method for favorable filling effect through thick film. Besides research in organic dyes, quantum dot sensitizers deserve more attention. Quantum dot sensitized solar cells possess relative low efficiency in liquid electrolyte and serious problem on stability.

In 2012, Kim and coworkers used $(CH_3NH_3)PbI_3$ as the sensitizer, and Spiro-OMeTAD as hole conductors to achieve an efficiency of up to 9.7% [29]. This efficiency is 48.3% higher than the liquid-state DSSC using $(CH_3NH_3)PbI_3$ as the sensitizer with an efficiency of 6.54%. The J_{sc} of the all-solid-state DSSCs using $(CH_3NH_3)PbI_3$ as the sensitizer reaches 17 $mA \cdot cm^{-2}$, which is much higher than that of all-solid-state DSSCs based on dye as the sensitizer.

Polythiophene is composing of high charge mobility, which is widely applied as hole transporting materials in solid-state DSSC. P3HT and PEDOT are common HTMs used in all-solid-state DSSCs. P3HT was also widely used in organic solar cells (OPV), in which P3HT acts not only as a HTMs but also as a light trapping materials. OPV using P3HT usually achieve an efficiency of 5% [30]. However DSSCs using P3HT got poor performances initially, the efficiency for devices based on N719 dye and P3HT is only about 1%, if no sensitizer is used in the device, the efficiency was only about 0.2%. In OPV, photogenerated carriers in P3HT can be quickly injected into the fullerene (C60 or C70). However in DSSCs, photogenerated carriers in P3HT do not seem to effectively inject into the dye or nanocrystalline TiO_2 film. In 2009, Zhu using D102 as a sensitizer and P3HT a hole transport material, and by treating the D102 sensitized nanocrystalline TiO_2 film with $Li(CF_3SO_2)_2N$ and 4-tert-butylpyridine, an efficiency of 2.63% was achieved, device without treatment got only an efficiency of 0.04% [31]. D102 absorption spectrum overlaps with the absorption spectrum of the P3HT, and therefore it is difficult to distinguish how much the IPCE value is created by P3HT. In 2009, Mor used the squaric acid dye SQ1 sensitized TiO_2 nanotubes as an anode and P3HT as a hole transport material to fabricate a solid state DSSC, which obtain a high efficiency of 3.8% [32]. The absorption spectral range of SQ1 is from 550 to 700 nm, which is complementary with the absorption spectrum of the P3HT. The contribution to photocurrent from SQ1 and P3HT can be directly seen from the IPCE. In 2011, Moon and coworkers [33] using YD2 dye as sensitizer and P3HT to fabricate a solid state DSSC and achieved an efficiency of 3.13%, in which the J_{sc} is up to 12.1 $mA \cdot cm^{-2}$. By comparing the absorption spectra and IPCE, the contribution to photocurrent from the P3HT and YD2 can be detected. In the same year, Zhang and coworkers [34] used D131 as a sensitizer together with P3HT as a hole transporting material to fabricate a solid-state DSSC and got an efficiency of 3.85%. It could be found from the IPCE that light to electron value above 550 nm is almost zero. Because P3HT still have strong absorption in the range from 550 to 645 nm, P3HT have no contribution to photocurrent for devices based on D131 and P3HT. Devices based on SQ1, YD2 and D131 exhibit different photovoltaic performance, this means different dyes have different reactions with P3HT. So it is necessary to conduct further studies on the mechanism of action between dye and P3HT in all solid-state DSSC. It is worth noting that quantum dots sensitizer have attracted more and more attention for all solid-state DSSCs based on P3HT. In 2010, Chang et al. used Sb_2S_3 quantum dots as sensitizer and P3HT as a hole transport material to fabricate solid state DSSC, which obtained a high efficiency of 5.13% [30]. IPCE reached more than 70% at spectral range from 350 to 530 nm, indicating high excitons separation efficiency for TiO_2/Sb_2S_3/P3HT system.

3.2.2 Monolithic all-solid-state DSSCs based on mesoscopic carbon CEs

It is very inspiring that all-solid-state DSSCs based on noble metal CEs have achieved an efficiency of over 10%. Unfortunately, the CEs of conventional solid-state DSSCs were fabricated by depositing noble metals such as gold or platinum on the solid-state medium. Obviously, this CE using high-cost metals is still an issue for its wide application since the vacuum deposition process is also highly energy consumptive. Thus, it is urgent to develop a low-cost CE for all-solid-state DSSCs. Porous carbon material is an excellent choice and the structure of monolithic all-solid-state DSSCs based on mesoscopic carbon CE is presented in Fig. 4. The fabrication procedures are as follows:

1) Laser scribing of the FTO conducting glass substrate;
2) Deposition of a layer of dense TiO_2;
3) Print a TiO_2 layer on the dense TiO_2 layer, and then sinter for 30 min at 450°C;
4) Print a ZrO_2 layer on the TiO_2 layer, after drying, print a carbon layer on the ZrO_2 layer, and then sinter for 30 min at 450°C;
5) Dye processing;
6) Pore filling of solid-state organic hole transport materials.

Compared with all-solid-state DSSCs based on noble metal CE, monolithic all-solid-state DSSCs based on carbon CE not only offer the prospect of being lower cost but also require a much simpler manufacturing process. For all-solid-state DSSCs based on metal CE, the

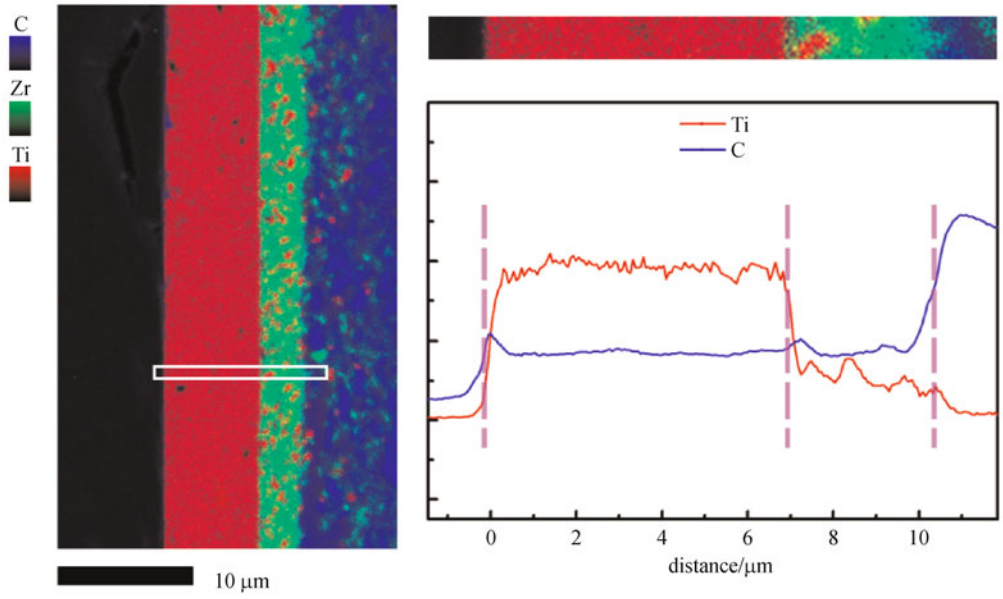

Fig. 8 Left: WDS mapping of the cross section of monolithic DSSC infiltrated with nanocomposite polymer electrolyte. Right: relative intensity of the Ti and C level across selected region of the device [19]

electrolyte is filled into the porous TiO_2 before the deposition of metal electrode. For all-solid-state DSSCs based on carbon CE, the electrolyte is filled into all the layers after the fabrication of carbon electrode. This avoids the employment of high vacuum condition and short circuit situation caused by depositing process. At the same time, the distance between working electrode and CE could be controlled precisely by the insulating layer. Thus, this design presents much better reproducibility for the performance of devices and is more suitable for large scale manufacturing.

However, a technical problem is caused by the carbon CE used for all-solid-state DSSCs. All along, researchers proposed that the reason that all-solid-state DSSCs could not obtain a high efficiency is the solid-state electrolyte could not be infiltrated the porous layer effectively. For all-solid-state DSSCs based on organic conductor Spiro-OMeTAD, the thickness of the TiO_2 layer is usually about 2 μm, which is far thinner than that of liquid-state electrolyte based DSSCs (about 12 μm). Besides the insulating layer, carbon layer should be thicker than 10 μm to obtain a comparable conductivity with FTO conducting glass substrate. In 2009, Han and coworkers [19] developed a low vacuum nanopore filling technique. Based on poly(ethylene oxide) (PEO)/poly(vinylidene fluoride) (PVDF) electrolyte system and platinized carbon CE, a monolithic all-solid-state DSSC was developed. According to the result, when the thickness of nanocrystalline TiO_2 layer, ZrO_2 insulating layer and carbon layer is below 60 μm, the filling method could obtain an effective filling of solid-state electrolyte as shown in Fig. 8. Less than 1 sun illumination, an efficiency of 3.65% was achieved with a high fill factor of 0.72. In 2012, Han group [35] reported a large-sized monolithic all-solid-state DSSC module using the similar material and structure, and achieved an efficiency of 2.57%.

PEO/PVDF nanocomposite electrolyte is based on I^-/I_3 redox couple. Thus, the carbon CE should present enough conductivity and electrochemical catalytic activity. The carbon CE is platinized for this requirement. But for the electrolyte of Spiro-OMeTAD, P3HT and other organic hole conductors, it is not necessary to obtain both conductivity and catalytic activity for the carbon electrode. Based on carbon black and graphite, in 2011, Han group used the dye of D102 and electrolyte of P3HT to assemble monolithic all-solid-state DSSCs and obtained an efficiency of 3.11% [14], which is much higher than that of devices based on the same dye and HTM and using vacuum deposited gold CE (2.65%) [26]. Compared with pure graphite based carbon CE, the addition of carbon black benefits the improvement of conversion efficiency. When the TiO_2 layer and ZrO_2 layer are 2 and 4 μm, respectively, an efficiency of 3.11% could be obtained for the carbon black/graphite CE based all-solid-state DSSCs. This is much higher than that of graphite CE based all-solid-state DSSCs (1.8%). Figure 9 presents the electrochemical impedance spectra (EIS) data of the devices [14]. In the high frequency range (1 MHz – 1 kHz), the arc corresponds to the electron exchange between P3HT and CE. In the low frequency range (500–0.4 Hz), the arc corresponds to the recombination between the electrons at the TiO_2 surface and P3HT. It is clear that the diameter of the arc for the graphite CE based device is much larger than that for graphite/carbon black CE based device in the high

frequency range. In contrast, the diameter of the arc is smaller in the low frequency range. This means the R_1 between graphite carbon CE and P3HT is much larger than that between graphite/carbon black CE and P3HT. And the R_2 between the TiO_2/P3HT of graphite CE based device is smaller than that of graphite/carbon black CE based device. Because the R_1 of graphite/carbon black CE based device ($9.7\,\Omega\cdot cm^2$) is smaller than that of graphite CE based device ($27.6\,\Omega\cdot cm^2$), the injection efficiency at the P3HT/CE interface of graphite/carbon black CE is higher than that of graphite CE based device, which leads a lager J_{sc}. In another aspect, for the graphite CE based DSSCs, because it is much more difficult for the electrons to transfer from CE to P3HT, the hole concentration in P3HT for graphite CE based device. This is beneficial for the electrons in the conduction band of TiO_2 activate with the holes in P3HT. This recombination reaction leads a decrease of the Fermi level of TiO_2, thus results a decrease in the V_{oc}. Considering the R_2 is smaller for graphite CE, the recombination life time for graphite/carbon black CE based device (3.5 ms) is longer than that of graphite CE based device (1.6 ms). Therefore, it could be concluded that the addition of carbon black into the carbon CE decrease the recombination between TiO_2 and P3HT. And graphite/carbon black CE could obtain a much better photovoltaic performance.

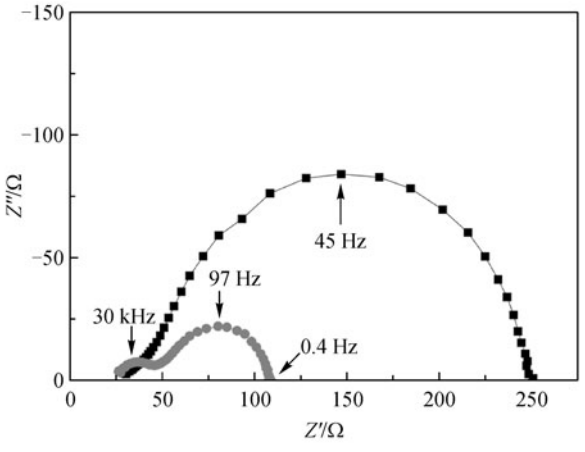

Fig. 9 Electrochemical impedance spectra (EIS) of P3HT-based monolithic DSSCs with different CEs: graphite CE (circle), graphite and carbon black CE (square) [14]

In 2013, Han group [36] employed Spiro-OMeTAD instead of P3HT to assemble monolithic all-solid-state DSSCs and obtained an efficiency of 4.1%. This value is comparable to that of noble metal CE based device. All these result indicates that carbon CE based monolithic DSSCs could be used for organic hole conductors. Besides, further research about CuI, CuSCN and $CsSnI_2$ is processing.

3.3 Module development

In 1996, Kay and Grätzel have proposed to fabricate monolithic DSSCs with continuous process [10]. The series connected module requires only one dimensional pattering of the coatings and thus lends to a continuous, conveyorized fabrication process (Fig. 10). Following manufacture of the glass substrate, a transparent conducting coat such as fluorine doped SnO_2 is applied by atmospheric chemical vapor deposition (CVD) onto the hot glass. The SnO_2 coating transparent conducting glass is then removed in parallel lines, by laser scribing, a technique routinely employed in the fabrication of amorphous silicon modules.

In the past decade, many researchers have focused on the commercial upscaling of DSSCs, and various approaches in enlarging the cell size have been attempted. In 2005, Dai group designed and tested DSSC modules with an overall efficiency of over 6% [37]. In 2009, an efficiency of 8.2% on a submodule of DSSC with series connected configuration was achieved by Han group [38]. For monolithic DSSCs, the unit cells could be connected in series, thus it is much simpler for this design to be enlarged. Pettersson, Meyer and Hinsch have completed abundant work on monolithic DSSC module design and fabrication [39–42]. In 2009, Meyer and coworkers reported a monolithic DSSC module (30 cm × 30 cm) consisting 35 inter-series connected unit cells as shown in Fig. 11(a). However, when connecting cells in series, it will be important to overcome these differences in cell performances to avoid significant energy losses. The solution would be more stringent control over the material components and process parameters, which goes against our ambition to develop a low-cost PV device. With parallel-connection, the energy losses will be smaller when the connected cells have similar V_{oc} but significant differences in J_{sc} and FF, i.e., the difference between the added energy from the maximum output of the individual cells and the energy output from the module when connecting the cells is smaller. Moreover, parallel-connection of cells eliminates the gradient of electrochemical potential between adjacent cells that may cause unwanted mass-transport between the electrolytes. Figure 11(b) shows a monolithic DSSC module consisting four parallel-connected unit cells (3.38 cm^2) [43].

In 2012, Han group first reported large-scale monolithic all-solid-state DSSC modules [35]. This design escapes from second conducting glass and noble metals used for CEs. Thus the material cost and fabrication process cost have been decreased largely. Assembled with solid-state electrolyte based on PEO/PVDF composite system, an efficiency of 2.57% is obtained. Since there is no risk of leakage of the electrolyte, the module becomes suitable for indoor applications, and is even portable. Figure 12(a) shows a digital image of a monolithic all-solid-state DSSC

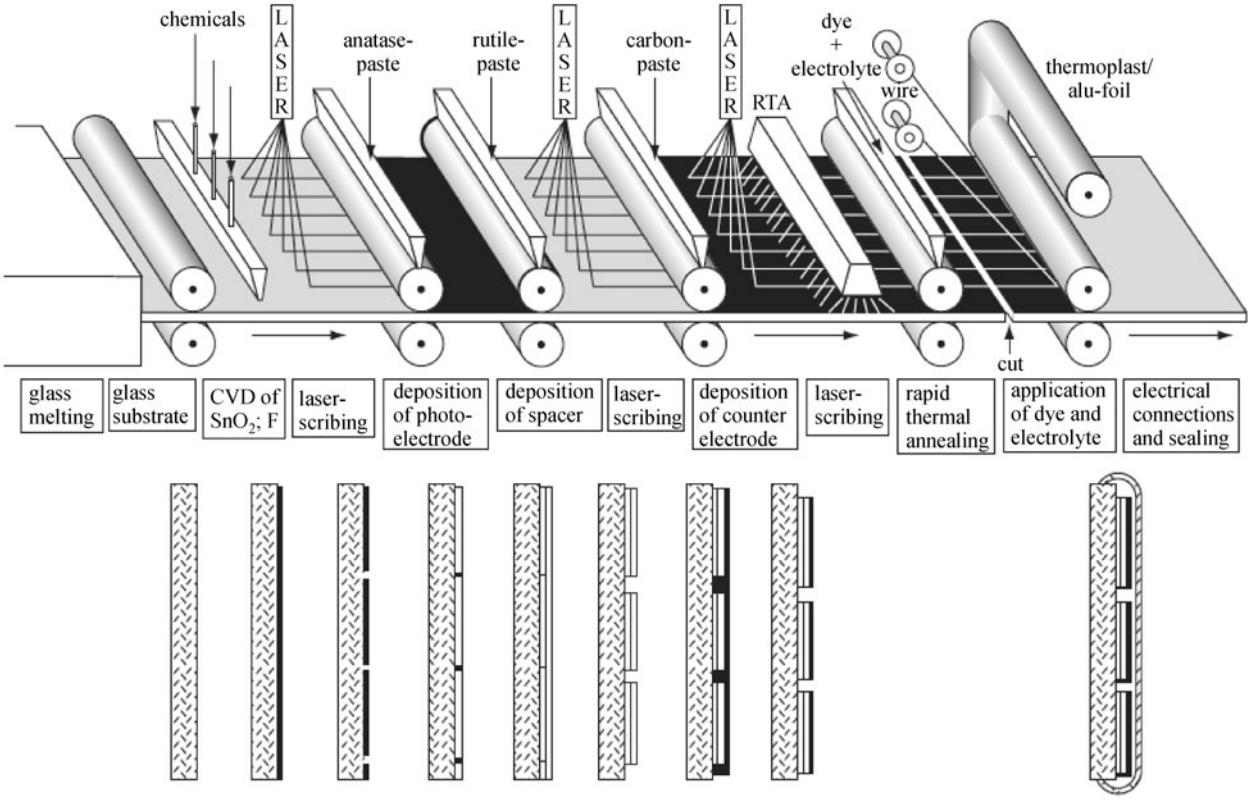

Fig. 10 Continuous process for fabrication of monolithic series connected DSSC modules [10]

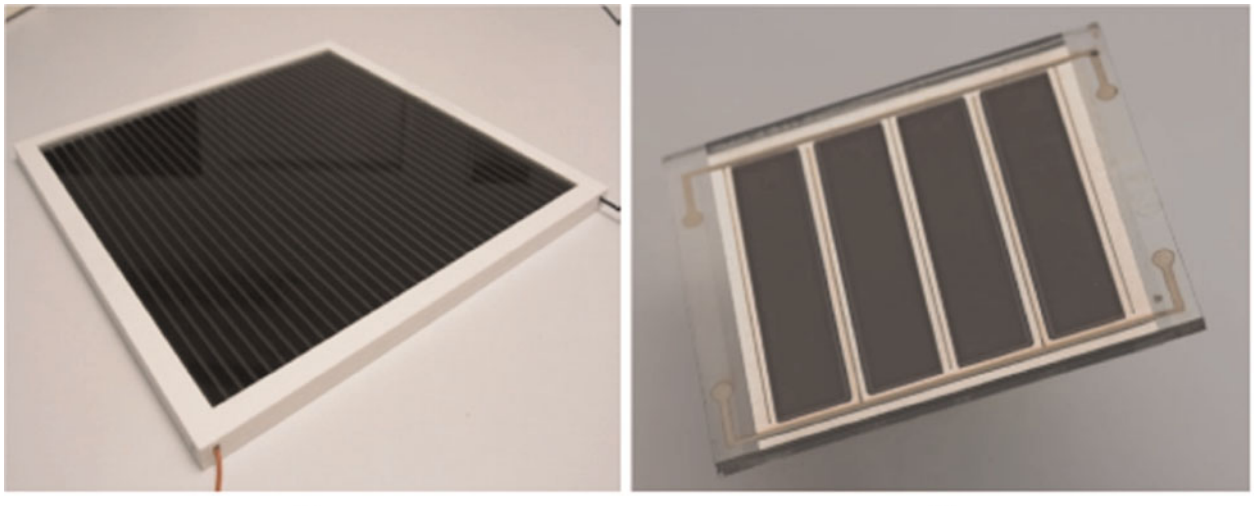

Fig. 11 (a) Monolithic DSSC module (30 cm × 30 cm) consisting 35 inter-series connected unit cells; (b) monolithic DSSC module consisting 4 parallel-connected unit cells (3.38 cm^2) [43]

module fabricated by experiment procedures that could drive an electric fan. This module works efficiently without any sealing process. Figure 12(b) shows the digital image of four solar panels consisting 80 monolithic all-solid-state DSSC modules fabricated by semi-auto process that could drive a LED display [35].

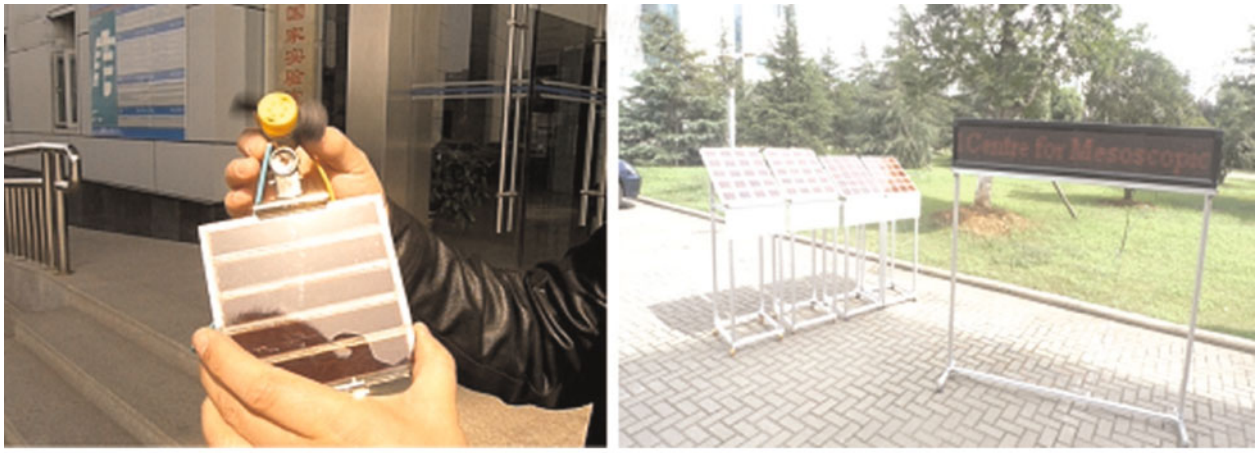

Fig. 12 (a) Monolithic all-solid-state DSSC module fabricated by experiment procedures that could drive an electric fan; (b) four panels consisting 80 monolithic all-solid-state DSSC modules fabricated by semi-auto process that could drive a LED display

3.4 Reproducibility and stability

Since all the layers of monolithic DSSCs are fabricated by screen printing, the fabricating procedures present excellent reproducibility. In 2007, Pettersson and coworkers attempted to improve the reproducibility of monolithic DSSCs [44]. As shown in Fig. 13, several devices are fabricated on a single conducting glass substrate. The average overall efficiency of the devices is 6.45% with a deviation of 0.18. Han and coworkers also completed some research on monolithic all-solid-state DSSCs. With a semi-automatic printer, the reproducibility is also satisfying. All these results indicate monolithic DSSC is very suitable for large scale manufacturing [45].

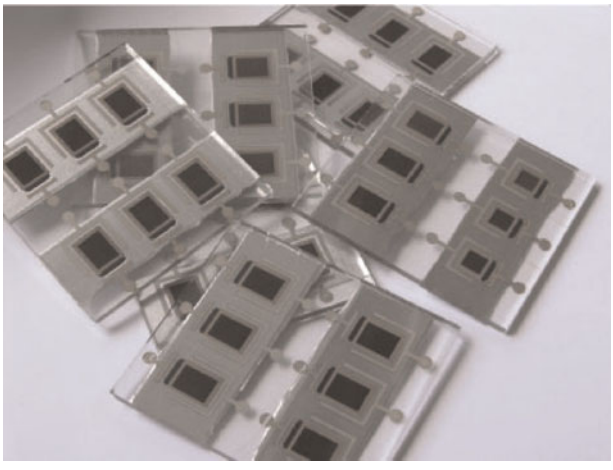

Fig. 13 Monolithic multicell with several individual cells [44]

As a device that would be exposed to sunlight and outdoor condition, the stability of DSSCs plays a key role for its commercialization. Preliminary research shows that the sealing issues affected the stability of DSSC devices significantly. To improve the stability of the devices, Kay and coworkers have investigated the influence of sealing process on the performance of the devices [10]. For traditional liquid-state DSSCs, the electrolyte employed acetonitrile as the solvent. Traditional sealing materials, such as epoxy resin, butyl rubber and silica gel, could not completely seal the device. The leakage of the liquid-state electrolyte would result in a rapid decay of the efficiency for DSSCs. Surlyn films are commonly used as sealing material for DSSCs in laboratory fabrication. The films melt at about 100°C. However, the devices sealed by Surlyn films would still leak electrolyte in the accelerating aging test at 70°C. This is caused by the ineffective cohesion between the conducting glass substrate and the Surlyn films, which makes the treatment of the surface of the conducting glass substrate very important. Petterson and Hinsch et al. have investigated the stability of monolithic DSSC modules detailedly, the tests of which considered illumination intensity, humidity, device condition and so on [41,46]. The result showed that the UV light affected the stability of the modules significantly. The UV illumination of modules without slowly degraded by a total of 4% over the testing period. The modules without UV filter, however, degraded much faster and were destroyed after 150 days. The initial decrease in maximum power of the modules without UV filter was mainly caused by reduced fill-factors. To clarify how different load conditions affect the stability, modules were illuminated (5000 lx) when operating at open-circuit, short-circuit and close to the maximum power point. The open-circuit configuration had a more negative influence and the module performance decreased by 20% over the testing period. Short-circuited modules or those operating close to the maximum power points, however, only decreased by 4% and thus, are more favorable operating configurations. At

long-term illumination at 20000 lx, the mean value of the maximum power decreased by 8% while at low light intensity (500 lx), the performance did not decrease over the testing period.

For monolithic all-solid-state DSSCs, there is no risk of leakage of the electrolyte. Han group [35] used hot melt film of ethylene vinyl acetate copolymer (EVA) and a plastic film of polyethylene terephthalate (PET) to seal the module fabricated with solid-state electrolyte. The result showed that moisture intrusion was an intrinsic problem for the stability of DSSC modules. Under high temperature and high humidity conditions (60°C, 85% RH), the performance of the module without sealing process diminished completely after the first 200 hours. In contrast, the module with sealing process presented much better stability against the highly humid environment, though a slight degradation of the efficiency of the module was observed. In the endurance test under a heat and cool cycle stress in the range of −10°C and 60°C, the V_{oc} and FF were almost stable, while the J_{sc} gradually decreased in the first 100 cycles and then stayed constant. After 200 cycles, the module retained over 92% of the initial conversion efficiency.

4 Future outlook

The ultimate goal of any photovoltaic technology is to achieve a cost-per-watt level that could compete against conventional fossil fuel technologies. In the past decade, silicon based solar cells have developed rapidly. The production cost has been decreased from about US$4.00 W^{-1} in 2005 to around US$0.66 W^{-1}. The module efficiency has been increased to 15%–20% and life times guarantee to 25 years. However, the electricity generation cost is much higher than that of conventional fossil fuel technologies [7].

DSSCs have been considered the most promising candidate of the next generation solar cells. Whether the commercialization of DSSCs could be realized depends on its cost performance and the market requirement. As the cost of silicon based solar cells decreased continuously these years, the superiority of traditional liquid-state DSSCs in cost has almost disappeared. In 2007, Grätzel group calculated the cost of traditional sandwich structure DSSC is US$90–116 m^{-2} based on the forecasted future materials costs [8]. To obtain a cost of US$0.66 W^{-1} comparable to silicon solar cells, the module efficiency should be 13.6%–17.6%. Through optimizing the dye, CE and electrolyte, the cost could be decreased. But in the last decade, the improvement of the efficiency in liquid-state DSSCs proceeded very slowly.

For the fabrication of DSSCs, the conducting glass substrates of FTO account for most of the production cost. But for monolithic DSSCs which only employ one substrate present much lower production cost. In 2009, Meyer and coworkers analyzed the production cost of liquid-state electrolyte and carbon CE based DSSCs [40]. The production cost is about US$62.5 m^{-2}. The overall module conversion efficiency needs to exceed 9.5% to make the cost below US$0.66 W^{-1}. At the same time, the cost for sealing accounts for about 26% of the production cost. Compared with monolithic liquid-state DSSCs, monolithic all-solid-state DSSCs eliminate the need for complicated sealing process, hole drilling, platinizing electrode, and so on. Thus the production cost is decreased a lot. If we just subtract the sealing cost, the production cost could be controlled below US$46.25 m^{-2}. Only if the efficiency reaches to 7%, the cost could be lower than US$0.66 W^{-1}. If the efficiency exceeds 10%, the cost would be lower than US$0.46 W^{-1}. This is much lower than that of the first generation silicon based solar cells and the second generation thin-film solar cells.

Through optimizing the sensitizer, spacer layer and CE, higher conversion efficiency could be obtained. With much lower production cost, monolithic all-solid-state DSSCs offers a promising prospect for wide application. In the long run, monolithic, all-solid-state, transparent, flexible DSSCs would dominate the market for DSSCs.

5 Conclusions

Monolithic all-solid-state DSSC based on mesoscopic carbon CEs and solid-state electrolytes offer the prospect of much lower production cost and long-term stability. However, further improvements of power conversion efficiency and stability of the devices and modules would be required before commercial production and applications. With great efforts devoted and more novel materials developed, the PCE of monolithic all-solid-state DSSCs has been continuously improved from 5% to over 15% in the last two years. It is highly expected that in the near future the PCE of monolithic all-solid-state DSSCs would be further improved to a higher level with high stability under the condition of low cost. With all the advantages of this design, monolithic all-solid-state DSSCs provides a promising path for the commercialization of DSSCs.

Acknowledgements The authors acknowledge the financial support by the National High Technology Research and Development Program of China (863 Program, No. SS2013AA50303), the National Natural Science Foundation of China (Grant No. 61106056) and Scientific Research Foundation for Returned Scholars, Ministry of Education of China.

References

1. O'Regan B, Grätzel M. A low-cost, high-efficiency solar cell based on dye-sensitized colloidal TiO_2 films. Nature, 1991, 353(6346): 737–740
2. Grätzel M. Photoelectrochemical cells. Nature, 2001, 414(6861):

338–344
3. Hagfeldt A, Boschloo G, Sun L C, Kloo L, Pettersson H. Dye-sensitized solar cells. Chemical Reviews, 2010, 110(11): 6595–6663
4. Chiba Y, Islam A, Komiya R, Koide N, Han L Y. Conversion efficiency of 10.8% by a dye-sensitized solar cell using a TiO_2 electrode with high haze. Applied Physics Letters, 2006, 88(22): 223505-1–223505-3
5. Han L Y, Islam A, Chen H, Malapaka C, Chiranjeevi B, Zhang S F, Yang X D, Yanagida M. High-efficiency dye-sensitized solar cell with a novel co-adsorbent. Energy & Environmental Sciences, 2012, 5(3): 6057–6060
6. Yella A, Lee H W, Tsao H N, Yi C Y, Chandiran A K, Nazeeruddin M K, Diau E W G, Yeh C Y, Zakeeruddin S M, Grätzel M. Porphyrin-sensitized solar cells with cobalt (II/III)-based redox electrolyte exceed 12 percent efficiency. Science, 2011, 334(6056): 629–634
7. Hardin B E, Snaith H J, McGehee M D. The renaissance of dye-sensitized solar cells. Nature Photonics, 2012, 6(3): 162–169
8. Kroon J M, Bakker N J, Smit H J P, Liska P, Thampi K R, Wang P, Zakeeruddin S M, Grätzel M, Hinsch A, Hore S, Wurfel U, Sastrawan R, Durrant J R, Palomares E, Pettersson H, Gruszecki T, Walter J, Skupien K, Tulloch G E. Nanocrystalline dye-sensitized solar cells having maximum performance. Progress in Photovoltaics: Research and Applications, 2007, 15(1): 1–18
9. Zhang Q F, Dandeneau C S, Zhou X Y, Cao G Z. ZnO nanostructures for dye-sensitized solar cells. Advanced Materials, 2009, 21(41): 4087–4108
10. Kay A, Grätzel M. Low cost photovoltaic modules based on dye sensitized nanocrystalline titanium dioxide and carbon powder. Solar Energy Materials and Solar Cells, 1996, 44(1): 99–117
11. Bach U, Lupo D, Comte P, Moser J E, Weissortel F, Salbeck J, Spreitzer H, Grätzel M. Solid-state dye-sensitized mesoporous TiO_2 solar cells with high photon-to-electron conversion efficiencies. Nature, 1998, 395(6702): 583–585
12. Melas-Kyriazi J, Ding I K, Marchioro A, Punzi A, Hardin B E, Burkhard G F, Tetreault N, Grätzel M, Moser J E, McGehee M D. The effect of hole transport material pore filling on photovoltaic performance in solid-state dye-sensitized solar cells. Advanced Energy Materials, 2011, 1(3): 407–414
13. Snaith H J, Moule A J, Klein C, Meerholz K, Friend R H, Grätzel M. Efficiency enhancements in solid-state hybrid solar cells via reduced charge recombination and increased light capture. Nano Letters, 2007, 7(11): 3372–3376
14. Wang H, Liu G H, Li X, Xiang P, Ku Z L, Rong Y G, Xu M, Liu L F, Hu M, Yang Y, Han H W. Highly efficient poly(3-hexylthiophene) based monolithic dye-sensitized solar cells with carbon CE. Energy & Environmental Sciences, 2011, 4(6): 2025–2029
15. Han H W, Liu W, Zhang J, Zhao X Z. A hybrid poly(ethylene oxide)/poly(vinylidene fluoride)/TiO_2 nanoparticle solid-state redox electrolyte for dye-sensitized nanocrystalline solar cells. Advanced Functional Materials, 2005, 15(12): 1940–1944
16. Lee M M, Teuscher J, Miyasaka T, Murakami T N, Snaith H J. Efficient hybrid solar cells based on meso-superstructured organo-metal halide perovskites. Science, 2012, 338(6107): 643–647
17. Chung I, Lee B, He J Q, Chang R P H, Kanatzidis M G. All-solid-state dye-sensitized solar cells with high efficiency. Nature, 2012, 485(7399): 486–489
18. Noh J H, Im S H, Heo J H, Mandal T N, Seok S I. Chemical management for colorful, efficient, and stable inorganic-organic hybrid nanostructured solar cells. Nano Letters, 2013, 13(4): 1764–1769
19. Han H W, Bach U, Cheng Y B, Caruso R A, MacRae C. A design for monolithic all-solid-state dye-sensitized solar cells with a platinized carbon counterelectrode. Applied Physics Letters, 2009, 94(10): 103102-1–103102-3
20. Skupien K, Putyra P, Walter J, Kozłowski R H, Khelashvili G. Catalytic materials manufactured by the polyol process for monolithic dye-sensitized solar cells. Progress in Photovoltaics: Research and Applications, 2009, 17(1): 67–73
21. Liu G H, Wang H, Li X, Rong Y G, Ku Z L, Xu M, Liu L F, Hu M, Yang Y, Xiang P, Shu T, Han H W. A mesoscopic platinized graphite/carbon black counter electrode for a highly efficient monolithic dye-sensitized solar cell. Electrochimica Acta, 2012, 69: 334–339
22. Hinsch A, Behrens S, Berginc M, Bönnemann H, Brandt H, Drewitz A, Einsele F, Faßler D, Gerhard D, Gores H, Haag R, Herzig T, Himmler S, Khelashvili G, Koch D, Nazmutdinova G, Opara-Krasovec U, Putyra P, Rau U, Sastrawan R, Schauer T, Schreiner C, Sensfuss S, Siegers C, Skupien K, Wachter P, Walter J, Wasserscheid P, Würfel U, Zistler M. Material development for dye solar modules: Results from an integrated approach. Progress in Photovoltaics: Research and Applications, 2008, 16(6): 489–501
23. Krüger J, Plass R, Cevey L, Piccirelli M, Grätzel M, Bach U. High efficiency solid-state photovoltaic device due to inhibition of interface charge recombination. Applied Physics Letters, 2001, 79 (13): 2085–2087
24. Krüger J, Plass R, Grätzel M, Matthieu H J. Improvement of the photovoltaic performance of solid-state dye-sensitized device by silver complexation of the sensitizer cis-bis(4,4′-dicarboxy-2,2′bipyridine)-bis(isothiocyanato) ruthenium(II). Applied Physics Letters, 2002, 81(2): 367–369
25. Schmidt-Mende L, Zakeeruddin S M, Grätzel M. Efficiency improvement in solid-state-dye-sensitized photovoltaics with an amphiphilic ruthenium-dye. Applied Physics Letters, 2005, 86(1): 013504-1–013504-3
26. Schmidt-Mende L, Bach U, Humphry-Baker R, Horiuchi T, Miura H, Ito S, Uchida S, Grätzel M. Organic dye for highly efficient solid-state dye-sensitized solar cells. Advanced Materials, 2005, 17(7): 813–815
27. Cai N, Moon S J, Cevey-Ha L, Moehl T, Humphry-Baker R, Wang P, Zakeeruddin S M, Grätzel M. An organic D-π-A dye for record efficiency solid-state sensitized heterojunction solar cells. Nano Letters, 2011, 11(4): 1452–1456
28. Burschka J, Dualeh A, Kessler F, Baranoff E, Cevey-Ha N L, Yi C Y, Nazeeruddin M K, Grätzel M. Tris(2-(1H-pyrazol-1-yl)pyridine) cobalt(III) as p-type dopant for organic semiconductors and its application in highly efficient solid-state dye-sensitized solar cells. Journal of the American Chemical Society, 2011, 133(45): 18042–18045
29. Kim H S, Lee C R, Im J H, Lee K B, Moehl T, Marchioro A, Moon S J, Humphry-Baker R, Yum J H, Moser J E, Grätzel M, Park N G.

Lead iodide perovskite sensitized all-solid-state submicron thin film mesoscopic solar cell with efficiency exceeding 9%. Scientific Reports, 2012, 2: 591

30. Chang J A, Rhee J H, Im S H, Lee Y H, Kim H J, Seok S I, Nazeeruddin M K, Grätzel M. High-performance nanostructured inorganic-organic heterojunction solar cells. Nano Letters, 2010, 10 (7): 2609–2612
31. Zhu R, Jiang C Y, Liu B, Ramakrishna S. Highly efficient nanoporous TiO_2-polythiophene hybrid solar cells based on interfacial modification using a metal-free organic dye. Advanced Materials, 2009, 21(9): 994–1000
32. Mor G K, Kim S, Paulose M, Varghese O K, Shankar K, Basham J, Grimes C A. Visible to near-infrared light harvesting in TiO_2 nanotube array-P3HT based heterojunction solar cells. Nano Letters, 2009, 9(12): 4250–4257
33. Moon S J, Baranoff E, Zakeeruddin S M, Yeh C Y, Diau E W G, Grätzel M, Sivula K. Enhanced light harvesting in mesoporous TiO_2/P3HT hybrid solar cells using a porphyrin dye. Chemical Communications (Cambridge), 2011, 47: 8244–8246
34. Zhang W, Zhu R, Li F, Wang Q, Liu B. High-performance solid-state organic dye sensitized solar cells with P3HT as hole transporter. Journal of Physical Chemistry C, 2011, 115(14): 7038–7043
35. Rong Y G, Li X, Ku Z L, Liu G H, Wang H, Xu M, Liu L F, Hu M, Xiang P, Zhou Z M, Shu T, Han H W. Monolithic all-solid-state dye-sensitized solar module based on mesoscopic carbon counter electrodes. Solar Energy Materials and Solar Cells, 2012, 105: 148–152
36. Xu M, Liu G H, Li X, Wang H, Rong Y G, Ku Z L, Hu M, Yang Y, Liu L F, Liu T F, Chen J Z, Han H W. Efficient monolithic solid-state dye-sensitized solar cell with a low-cost mesoscopic carbon based screen printable counter electrode. Organic Electronics, 2013, 14(2): 628–634
37. Dai S Y, Wang K J, Weng J, Sui Y F, Huang Y, Xiao S F, Chen S H, Hu L H, Kong F T, Pan X, Shi C W, Guo L. Design of DSC panel with efficiency more than 6%. Solar Energy Materials and Solar Cells, 2005, 85(3): 447–455
38. Han L T, Fukui A, Chiba Y, Islam A, Komiya R, Fuke N, Koide N, Yamanaka R, Shimizu M. Integrated dye-sensitized solar cell module with conversion efficiency of 8.2%. Applied Physics Letters, 2009, 94(1): 013305-1–013305-3
39. Meyer T, Martineau D, Azarn A, Meyer A. All screen printed dye solar cell. Organic Photovoltaics VIII, 2007, 6656: 65608-1–65608-11
40. Meyer T, Scott M, Azam A, Martineau D, Oswald F, Narbey S, Laporte G, Cisneros R, Tregnano G, Meyer A. CleanTechDay 3rd Generation Photovoltaics, CSEM, Basel, 18 August 2009
41. Pettersson H, Gruszecki T. Long-term stability of low-power dye-sensitised solar cells prepared by industrial methods. Solar Energy Materials and Solar Cells, 2001, 70(2): 203–212
42. Pettersson H, Gruszecki T, Johansson L H, Johander P. Manufacturing method for monolithic dye-sensitised solar cells permitting long-term stable low-power modules. Solar Energy Materials and Solar Cells, 2003, 77(4): 405–413
43. Pettersson H, Gruszecki T, Schnetz C, Streit M, Xu Y H, Sun L C, Gorlov M, Kloo L, Boschloo G, Haggman L, Hagfeldt A. Parallel-connected monolithic dye-sensitised solar modules. Progress in Photovoltaics: Research and Applications, 2010, 18(5): 340–345
44. Pettersson H, Gruszecki T, Bernhard R, Haggman L, Gorlov M, Boschloo G, Edvinsson T, Kloo L, Hagfeldt A. The monolithic multicell: a tool for testing material components in dye-sensitized solar cells. Progress in Photovoltaics: Research and Applications, 2007, 15(2): 113–121
45. Rong Y G, Han H W. Monolithic quasi-solid-state dye-sensitized solar cells based on graphene modified mesoscopic carbon-counter electrodes. Journal of Nanophotonics, 2013, 7(1): 073090
46. Hinsch A, Kroon J M, Kern R, Uhlendorf I, Holzbock J, Meyer A, Ferber J. Long-term stability of dye-sensitised solar cells. Progress in Photovoltaics: Research and Applications, 2001, 9(6): 425–438